Published in final edited form as:
Neuroscience. 2010 January 13; 165(1): 252–264. doi:10.1016/j.neuroscience.2009.09.066.

Intra- and Inter- Subject Variability of High Field fMRI Digit Maps in Somatosensory Area 3b of New World Monkeys

Na Zhang[1,7,8], **Feng Wang**[1,2], **Greg H. Turner**[1,2,¶], **John C. Gore**[1,2,3,4,7], **Malcolm J. Avison**[1,2,5,6], and **Li M. Chen**[1,2,*]

[1] Institute of Imaging Science, Vanderbilt University

[2] Department of Radiology & Radiological Sciences, Vanderbilt University

[3] Department of Biomedical Engineering, Vanderbilt University

[4] Department of Molecular Physiology and Biophysics, Vanderbilt University

[5] Department of Pharmacology, Vanderbilt University

[6] Department of Neurology, Vanderbilt University

[7] Department of Physics and Astronomy, Vanderbilt University

[8] Department Electrical and Computer Engineering, Clarkson University

Abstract

This study evaluates the intra- and inter- subject variability of digit maps in area 3b of anesthetized squirrel monkeys. Maps were collected using high field Blood Oxygenation Level Dependent (BOLD) fMRI. BOLD responses to individual digit stimulations were mapped and their response properties (location, area of activation, % signal change, time to peak response) were compared within and across imaging sessions separated by up to 20 months. During single digit stimulation using a block design, the spatio-temporal response of the BOLD signal for individual runs within and across sessions and animals was well conserved, with a time to peak BOLD response of 20 ± 4 sec. The variability in the center of BOLD activation in area 3b was 0.41 ± 0.24 mm (mean ± SD) across individual 5–7 minutes runs within a scanning session and 0.55 ± 0.15 mm across sessions. The average signal change across all animals, runs and sessions was 0.62 ± 0.38 %, and varied 32% within and 40% across sessions. In a comparison of the stability and reproducibility of the area of single digit activation obtained using three approaches, use of a fixed statistical threshold ($p<10^{-5}$) yielded an average area of 4.8 ± 3.5 mm^2 (mean ± SD), adaptive statistical thresholding 1.32 ± 1.259 mm^2 (mean ± SD), and combined fixed statistical and adaptive BOLD signal amplitude 4.4 ± 2.5 mm^2 (mean ± SD) across image runs and sessions. The somatotopic organization was stable within animals across sessions, while across animals, there was some variation in overall activation pattern and inter-digit distances. These results confirm that BOLD activation maps of single digits in area 3b as characterized by activation center, signal amplitudes, and temporal profile are very stable. The

*Corresponding Author: Li Min Chen, M.D., Ph.D., Department of Radiology and Radiological Science, Institute of Imaging Science, Vanderbilt University, Nashville, TN, USA, Phone: 615-9367069, Fax: 615-322-0734, Limin.chen@vanderbilt.edu.
¶Author's current address: Keller Center for Imaging Innovation, Barrow Neurological Institute/Saint Joseph's Hospital and Medical Center, 350 W. Thomas Road, Phoenix, AZ 85013

Section editor: sensory system. Dr. Richard Weinberg, University of North Carolina, Department of Cell Biology and Anatomy, CB 7090, Chapel Hill, NC 27599, USA

activation sizes determined by various criteria are the most variable measure in this preparation, but adaptive statistical thresholding appears to yield the most stable and reproducible maps. This study serves as a baseline assessment of the limits imposed on the detection of plastic changes by experimental variations of the digit BOLD fMRI activation maps in normal animals, and as an indicator of the likely performance limits in human studies.

Keywords

high field functional MRI; primates; somatosensory cortex; digits; topography

1. Introduction

fMRI can image brain activity across a wide range of distances and scales, from whole brain networks to cortical columns in humans, and in anesthetized and awake animals. By virtue of its non-invasiveness, fMRI is particularly well suited for studying brain function longitudinally and for mapping plastic changes in the central nervous system. Several studies have confirmed the ability of high field fMRI, using both endogenous blood oxygenation level dependent (BOLD) and exogenous intravascular contrast, to resolve sub-millimeter functional organization in the CNS, including fine scale ocular dominance and orientation modules in primary visual cortex (Menon and Goodyear, 1999; Fukuda et al., 2005; Fukuda et al., 2006; Moon et al., 2007; Goense and Logothetis, 2008; Yacoub et al., 2008), single digit tactile response in somatosensory cortices (Chen et al., 2007; Zhang et al., 2007; Meier et al., 2008; Nelson and Chen, 2008; Schweizer et al., 2008), and odor maps in olfactory cortex (Kida et al., 2002; Schafer et al., 2006; Courtine et al., 2007). These results suggest that high field BOLD fMRI can be used to follow the spatio-temporal trajectory of functional reorganization, such as that observed following spinal cord injury for example see (Jones, 2000; Kaas, 2000; Kaas et al., 2007), with sub-millimeter resolution. To do so, it is necessary to establish the intra-subject stability and inter-subject variability of BOLD fMRI maps of the particular system to be studied.

The stability and variability of BOLD signal have been investigated previously within and across subjects both in humans and animals (Moser et al., 1996; Rombouts et al., 1998; Tegeler et al., 1999; van Gelderen et al., 2005; Schafer et al., 2006; Leontiev and Buxton, 2007; Yoo et al., 2007). In humans, while functional maps have generally been reproducible, variations in location, activation volume and temporal profiles have been observed in repeat fMRI mapping studies in visual, motor, and somatosensory cortices (Rombouts et al., 1998; Tegeler et al., 1999; Waldvogel et al., 2000; Salli et al., 2001; Fernandez et al., 2003; Neumann et al., 2003; Tjandra et al., 2005; van Gelderen et al., 2005; Harrington et al., 2006; Menz et al., 2006; Costafreda et al., 2007; Yoo et al., 2007; Whalley et al., 2009) though the origin of these variations are not well understood. Excellent intra-subject reproducibility of high field high-resolution odor maps has been demonstrated within a single imaging session in rats (Schafter et al 2006). However, the long-term stability of high resolution fMRI maps, particularly in somatosensory cortices of non-human primates is less well known (Chen et al., 2005). The aim of the present study was to establish the longitudinal intra-subject stability and inter-subject variability of fMRI activation maps of digit representations in primary somatosensory cortex (area 3b) of squirrel monkeys collected at sub-millimeter spatial resolution. This region was chosen because electrophysiological and optical imaging studies have consistently identified somatotopically organized discrete representations of individual digits in area 3b that are readily activated by physiologically relevant somatosensory stimuli, and which undergo significant functional reorganization following focal loss of sensory inputs, such as can occur in cervical spinal cord injury.

In primates, somatosensory area 3b plays an important role in touch perception, and it contains a fine representation of the body surface. The somatotopic organization of digit representations in area 3b of non-human primates has been well established with various invasive techniques such as microelectrode receptive field mapping, histology (Nelson et al., 1980; Sur et al., 1982; Pons et al., 1987; Reed et al., 2008), optical imaging of intrinsic signal (Tommerdahl et al., 1999; Chen et al., 2001; Tommerdahl et al., 2002; Chen et al., 2003), and noninvasive fMRI (Chen et al., 2007; Zhang et al., 2007). Somatotopically, each digit occupies about 1 mm^2 cortical area in area 3b of squirrel monkeys. Functionally, neurons in area 3b representing the digits typically have small receptive fields (e.g. limited to a finger pad), and are organized in columnar structures (Mountcastle, 1957; Sur et al., 1984; Favorov and Whitsel, 1988a, 1988b; Kohn et al., 1997; Mountcastle, 1997, , 2003; Friedman et al., 2004). When cortical responses to tactile stimuli have been mapped using hemodynamic signals in anesthetized monkeys (e.g. optical imaging of intrinsic signal), comparable activations of 1 mm^2 with limited overlap between adjacent digit responses have been observed (Chen et al., 2001; Chen et al., 2003, , 2005), supporting the notion that functional mapping using a hemodynamic signal corresponds well spatially to local neuronal activities (Yang et al., 1997; Disbrow et al., 1999; Tommerdahl et al., 1999; Disbrow et al., 2000; Logothetis et al., 2001; Tommerdahl et al., 2002; Lauritzen and Gold, 2003; Chen et al., 2007; Vanzetta and Grinvald, 2008). Furthermore, the close correspondence of maps obtained using the BOLD mapping signal to those derived from optical imaging and electrophysiological mapping in the same animal has also been demonstrated (Chen et al., 2007). All three approaches reveal the same orderly and separable single digit somatotopic organization. These results are in contrast to reports of the spatial extent of digit representation overlapping observed in human primary somatosensory cortex (e.g. subregion area 3b) (Gelnar et al., 1998; Maldjian et al., 1999; Krause et al., 2001; van Gelderen et al., 2005; Nelson and Chen, 2008; Schweizer et al., 2008), and may reflect the lower spatial resolution of the earlier studies. Taken together, these studies suggest that high field fMRI can map cortical and subcortical functional structures with submillimeter resolution, permitting longitudinal quantitative assessments of functional plastic changes of cortical and subcortical structures in primates non-invasively with submillimeter spatial resolution. However a quantitative measure of the variability and reproducibility of these maps, particularly across multiple mapping sessions in a longitudinal study, is an essential pre-requisite for distinguishing and characterizing functional reorganization. This is the goal of the present study, and the data presented serve as a baseline assessment of the limits imposed by fMRI mapping methods on the detection of plastic changes in normal animals and after experimental interventions, as well as suggesting the potential sensitivity available in human studies.

2. Methods

2.1 Animal Preparation

Six monkeys were used in this study. Each animal was sedated with ketamine hydrochloride (10mg/kg)/atropine (0.05mg/kg) and mechanically ventilated with isoflurane anesthesia (0.5–1.1%) delivered in a 30:70 O_2:NO_2 mixture. After intubation, the animals were placed in a custom-designed MR cradle and their heads secured with ear and head bars. Saline was infused intravenously (2–3ml/kg/hr) throughout the imaging session to prevent dehydration. SpO2 and heart rate (Nonin, Plymouth, MN), ECG, ET-CO2 (22–26 mmHg; Surgivet, Waukesha, WI), and respiratory pattern (SA instruments, Stony Brook, NY) were monitored. Rectal temperature was monitored (SA instruments) and maintained (37.5–38.5 °C) via a combination of a circulating water blanket (Gaymar Industries, Orchard Park, NY) and a flow of warm air (SA instruments). Real time monitoring of the animal was maintained from the time of induction of anesthesia until full recovery. All procedures were in compliance with and approved by the Institutional Animal Care and Use Committee of Vanderbilt University.

2.2 Stimulus Protocol

Fingers were secured by gluing small pegs to the fingernails and fixing these pegs firmly in plasticine, leaving the glabrous surfaces available for vibrotactile stimulation. Piezoceramic actuators (Noliac, Kvistgaard, Denmark) delivered a vertical indentation of a 2 mm diameter probe with 0.34 mm displacement to individual distal fingerpads. The piezoactuators were driven by Grass stimulators (Grass-Telefactor, West Warwick, RI) at a rate of 8 Hz with 30 ms pulse duration. Five to seven alternating 30 s blocks of baseline and vibrotactile stimulation were delivered per imaging run. The MR scanner controlled the timing of the stimulus blocks.

2.3 MR Methods

All scans were performed on a 9.4T 21-cm narrow-bore Varian Inova magnet (Varian Medical Systems, Palo Alto, CA) using a 3-cm surface transmit-receive coil positioned over the somatosensory cortex. Scout images using a gradient-echo sequence were used to define a brain volume covering the primary somatosensory cortex (SI) and to plan oblique coronal slices for structural and functional images (See Fig 1 of Chen et al. 2007 for details). After shimming over this volume, T2*-weighted gradient echo structural images (repetition time (TR), 200 ms; echo time (TE), 14 ms, three slices, 512X512 matrix; 78 X 78 X 2000 μm resolution) were acquired to identify venous structures on the cortical surface, that were used to locate SI cortex and provide structural features for coregistration of MRI maps obtained across imaging sessions on different sessions. FMRI data were acquired from the same slice using a gradient echo planar (GE-EPI) sequence (TE=16 ms; TR=1.5 sec; 64 X 64 matrix; 625 X 625 X 2000 μm resolution). The TR on individual scans was adjusted to match the ventilation rate to minimize respiration-induced signal variations in the functional time-courses. Typically an experiment lasted about 6 hours, so the functional images acquired within the same experiment (e.g. in response to the same digit stimulation) could be several hours apart.

2.4 fMRI Data Analysis

Reconstructed images were imported into Matlab (Mathworks, Natick, MA) for analysis. The time courses of the EPI data were drift corrected using a linear model and temporally smoothed with a low-pass filter. The correlation of each functional time course to a reference waveform and the positive BOLD percentage signal change were calculated. Activation maps were interpolated to 512 × 512 to match the structural images, and for each animal the activated voxels were overlaid on the corresponding structural images for display and calculation. All maps are displayed as single condition activation maps.

2.5 Alignment of BOLD activation maps across imaging sessions

To calculate the spatial shifts of activation centers across imaging sessions, we first aligned anatomical images acquired from each imaging session using an automatic rigid coregistration algorithm (Hill et al., 1991; Chen et al., 2002). An example of two aligned T2* weighted structural images are shown in Figure 1A, B. The T2* weighting reveals venous structures (thin dark lines, red arrows) that were used together with anatomical features (central and lateral sulci, green arrows), as coregistration landmarks. Typically we chose as landmarks more than 8 points surrounding the region of interest (digit representations), selected from anatomical images acquired in the different imaging sessions. These were then input into a point-based registration algorithm (implemented in MATLAB) for automatic transformation. The landmarks were selected without *a priori* knowledge of the location of functional activations. For each pair of anatomical MRI images, the registration transformation between these two sets of coordinates was then applied to one activation image, thereby co-registering the fMRI images across sessions (Hill et al., 1991; Chen et al., 2002).

2.6 Stability measures

Within one imaging session (day), we first generated a single condition (stimulus versus baseline) activation map for each imaging run at a fixed statistical threshold. Generally each digit representation was mapped three to five times to increase the signal noise ratio. To calculate the variability in the location of the BOLD activation across runs, the center of digit activation was determined by the x–y coordinate of the voxel that had the highest statistical significance. We also generated an average activation map for each session by averaging weighted statistical maps across runs. The distances between the center of the averaged activation map and center locations of the same digit across individual imaging runs were calculated and used as a measure of the variation across runs. The variability in location across sessions (days) was measured in the same way, comparing the location in average activation maps for a given session, with that in the grand average across sessions after image coregistration.

For fMRI data, there is still no consensus on what methods or criteria are most appropriate to quantify the spatial extent of activation. Therefore, in this study, we compared three different methods for defining the area of activation: 1) fixed statistical thresholding; 2) adaptive statistical thresholding; 3) dual threshold (statistical threshold followed by adaptive % signal change threshold). In the fixed threshold method, activated voxels were determined by thresholding voxels to a fixed statistical significance value (e.g. $p<10^{-5}$). With the adaptive threshold method (Moser et al., 1996; Krause et al., 2001), activated voxels were calculated in each run by adjusting the acceptance threshold (p value) to have a $p< p_{min}\times 10^{2}$ where p_{min} is the lowest p value in that imaging plane, as shown in Figures 2 and 3. For dual thresholding, voxels were first thresholded at a fixed statistical threshold ($p< 10^{-3}$), and those passing the statistical threshold were then thresholded again at % signal change greater than or equal to 20% of the maximum BOLD signal within that image plane.

To calculate the time course and amplitude of BOLD signal change, a common ROI (same voxel size and location) was defined by the average area of 3b activation within or across sessions, and then the BOLD signal profiles within the ROI were calculated for each run or session as appropriate. Time to peak measurements were calculated from the averaged time courses. The variation of percentage signal change was calculated as (%A − %B)/(%A+%B).

12 imaging sessions generated from six monkeys (four animals had two image sessions, one animal had 3 sessions and 1 animal had one session) were included in the analysis. Across the five animals that were scanned repeatedly, the inter-session intervals were 2, 2, 8 weeks, 5 or 20 months, respectively. A typical imaging session lasted 4–6 hrs. Within each imaging session, either three (d2, d3, d4) or four (D1, D2, D3, and D4) individual digits were mapped using single digit stimulation. Online correlation analysis of each run was conducted during the imaging session to guide the optimization of anesthesia level. Individual runs were included in subsequent analyses if they met the following minimal quality criteria: 1) structured activations consistent with prior optical imaging studies (e.g. Chen et al., 2001 and 2003) were revealed in area 3b when correlation maps were thresholded at a minimal $p<10^{-5}$ uncorrected for multiple comparisons; 2) ROI analysis revealed a BOLD signal response clearly distinguishable from any baseline fluctuations. Microelectrode mapping validated the location of area 3b. Imaging sessions that detected at least two repeatable BOLD responses for each digit stimulation condition were included in quantitative analysis.

3. Results

Intra-subject stability of single digit activation maps

a) Within imaging sessions

Center of activation: We first measured the variation in the distance between the centers of BOLD activations for each run within one imaging session. Examples from three monkeys (M1–M3) are shown in Figure 2. Consistent with our earlier study (Chen et al., 2007), we observed focal activations in each run during single digit 8 Hz vibrotactile stimulation (Figure 2B, C: D3 in M1; H, I: D3 in M2; N, O: D4 in M3). When adaptive thresholding was applied ($p< p_{min}\times 10^2$), we observed similar sized activations in area 3b in all three animals. In addition, average maps (Figure 2D, J, and P; red-yellow patches) were also generated to illustrate the effects of across run averaging on activation location and size. When anatomically coregistered functional images from individual runs were overlaid on average activation maps, we observed excellent co-localization of activations across single runs (green and blue outlines), and with the activation maps calculated by averaging all runs (Figure 2E, K, and Q). In M1, the center of activation (defined as the voxel with the most significant p value) obtained in M1 differed by 0.55 mm between runs 1 and 2, and this was reflected also in a shift of the activation boundary (Fig. 2E). The between run differences in activation center were much smaller for M2 (0.078 mm, Fig. 2K) and M3 (0.175 mm, Fig. 2Q), and in both these animals the activation boundaries across runs were very similar. The mean pair-wise distance between all pairs of single run activations within a session, averaged across all runs and all monkeys was 0.41 ± 0.24 mm (mean ± SD; 5 animals, 11 sessions).

Percentage BOLD signal change: We next evaluated the stability of the fractional BOLD signal change across imaging runs within a single session, using the average signal change within the region of interest (ROI) in area 3b identified from the activation map generated by combining all runs in the session. The peak percentage change of BOLD signal in each run of 5–7 alternating blocks of baseline and stimulation, and the averaged BOLD signal across all runs for each animal are also illustrated (Fig 2F, L, R, for M1–M3 respectively). Average percentage BOLD signal change within and across runs within a session ranged from 0.35% (M3 run 1) to 0.9% (M1 run1) within a single run, and 0.4% (M3) to 0.6% (M1, M2) for the average across runs. Across animals, the fractional signal changes within a session varied 32%.

b) Across imaging sessions (2 weeks – 20 months)

Center of activation: In contrast to the calculation of changes in center of activation within one imaging session where all the cross-run activation maps are coherently registered into one imaging space, an intermediate co-registration step was required for quantifying differences in activation centers across sessions. Imperfections in this step can introduce additional variability. As expected, more variations were present in activation pattern (shape), size, and locations during single digit stimulation across image sessions. Figure 3 summarizes four examples (out of five monkeys studied longitudinally) of activation maps (determined by adaptive threshold) during two different imaging sessions separated by 2 weeks (M3, M4), 5 months (M5) and 20 months (M2). In comparison to the within session measurements, the variability in location of the activation centers across sessions, measured as the distance between the most significant voxel in the session 1 and session 2 average activation maps, was slightly greater (0.55 ± 0.15 mm; n=5 animals). Finally, there was considerably more variation across sessions in the patterns of activation beyond area 3b (Figure 3C and D). We attribute this to the greater sensitivity of higher order sensory areas to subtle variations in anesthesia within and across sessions (Chen et al., 2001;Chen et al., 2005;Friedman et al., 2008).

Area extent of activation: Three different methods were assessed to quantify the size of the activation area. For a given fixed threshold, the area of single digit activation in area 3b across

runs in all sessions (n = 49 total) in all animals varied widely (Figure 4), reflecting the variations in signal to noise ratio across imaging runs and sessions. At a relatively conservative fixed threshold of $p<10^{-5}$ (uncorrected), the average area for single digit activation was 4.8 ± 3.5 mm^2, i.e. a variation of 72% (SD/mean). When, we applied the dual threshold of fixed statistical ($p<10^{-3}$) followed by adaptive signal amplitude (>20 % of maximum signal change), the mean area of activation for single digits was 4.4 ± 2.5 mm^2 with a variation of 57%. Finally, the adaptive statistical threshold method resulted in a smaller average activation size of 1.32 ± 1.25 mm^2 (mean ± SD), but with a larger variation of 95%. Thus of the three approaches, the dual threshold approach (fixed statistical-adaptive signal amplitude) had the lowest variability, while the adaptive statistical threshold yielded a more focal area of activation whose boundaries were most reproducible from run to run and across sessions, with activation areas that most closely resembled the ~1 mm^2 area observed for digit representations in area 3b by optical imaging and electrophysiological studies in vivo and post mortem myelin staining.

Temporal profile of BOLD signal change: We next evaluated the stability of the BOLD signal time course in area 3b across imaging sessions on different days. Figure 5 compares the mean timecourses of the BOLD signal changes (averaged across baseline-stimulus epochs and runs) from the same ROI (defined by the area 3b activation in session 1) in two sessions separated by 2 weeks (M3, M4), 5 months (M5) and 20 months (M2). The temporal profiles of the BOLD signal in area 3b were typical of responses to long duration stimuli (30 sec), reaching a peak at an average of 20 ± 3.9 sec after stimulus onset, and showing delayed post-stimulus undershoot. There were no consistent patterns of difference between the first and second sessions across all animals' studies. Thus for the two animals restudied at 2 weeks (M3, M4), there were small differences in the early response between the session 1 and session 2 time courses-M3's early response was stronger in session 1, M4's in session 2-but there was no difference in post-stimulus undershoot (Fig 5C, D). Conversely, in M5 and M2, restudied at 5 and 20 months, there were no significant differences in the positive BOLD time course between sessions but for both animals post-stimulus undershoots were smaller and briefer for session 2 (Fig 5A, B). This variability probably reflected imperfect filtering of small run to run fluctuations in the amplitude of baseline BOLD fluctuations unrelated to the stimulus. The average 0.62% BOLD signal amplitude change is consistent with our previous report in this experimental model system (Chen et al., 2007). Across animals, the cross-session variation of BOLD signal was ~40%, with no consistent trends across animals for either an increase or decrease in later sessions. Figure 6 summarizes the stimulus-associated % signal changes averaged across runs and days (sessions) (mean ± SD) for all animals (n=6). These data confirm the stability of the BOLD signal time course across imaging sessions separated by as long as 20 months (M2).

In sum, intra-subject single digit BOLD activation maps as characterized by center of activation, percentage signal amplitude, and temporal profile of signal were very stable across runs and sessions.

Inter-subject variability of digit somatotopic representation in area 3b

Previous mapping studies have reported some inter-subject variability of digit representations in monkey primary somatosensory cortex (Juliano and Whitsel, 1985; Merzenich et al., 1987). We therefore evaluated the ability of BOLD fMRI mapping to reveal consistent inter-subject variations in the somatotopic organization of digit activations in area 3b. Time constraints imposed in each imaging session limited our mapping to the distal fingerpads of digits 2 to 4 (D2–D4). Figure 7A–F compares the somatotopic maps for each of the six animals studied, overlaid on their corresponding anatomic images. For illustration purposes, adaptive statistical thresholds resulting in non-overlaying adjacent digit activations were used. Although the general fingerpad topography, with lateral to medial ordering of D2–D4 representations,

was similar in all animals, there were clear inter-subject variations (Fig. 7A–F). Nonetheless, the inter-subject variations were small compared with the general somatotopic organization, and the mean inter-digit distances measured as the distance between centers of activation of individual digits in each animal (Fig. 7G). Thus the average distances between activation centers were: D2–D3 1.25 ± 0.01 mm (n = 4); D3–D4 1.07 ± 0.4 mm (n = 6); D2–D4 2.04 ± 0.55 mm (n = 5). Again, consistent with previous fMRI, optical imaging of intrinsic signal (OIS) and electrophysiological mapping studies (Sur et al., 1982; Chen et al., 2001; Chen et al., 2003; Chen et al., 2007) in this species, the average distance between non-adjacent digits was roughly twice that between adjacent digits. These data confirm and provide normative information regarding inter-individual variations in the somatotopic representation of individual digits at fine scale.

4. Discussion

Summary

In this study, using endogenous BOLD contrast fMRI, we have confirmed the long-term stability of intra-subject digit representation maps, and examined the inter-subject variability of somatotopic maps of the distal finger pads in primary somatosensory cortical area 3b during vibrotactile fingerpad stimulation. Extending our previous findings (Chen et al 2007), we have demonstrated that the spatial and temporal features of the BOLD fMRI mapping signal, including center location of activation, peak % signal change, and time to peak, were stable over a period of up to 20 months. The sizes of activation determined by various methods were the most variable measures. A relatively conservative fixed statistical threshold generated the largest single digit activation areas in area 3b, with significant variability across runs and sessions, adaptive statistical thresholding generated ~ 1 mm^2 activations most congruent with the areas identified by optical imaging and myelin staining, but with the greatest % variability across runs and sessions, and the dual threshold (fixed statistical, adaptive signal amplitude) areas closer to those defined by the fixed statistical threshold, but with the lowest variability. This study confirmed the general similarity of digit somatotopy in area 3b across the six animals studies, but also revealed significant inter-individual variations. Finally, this study quantified the sensitivity, spatial resolution and stability limits of high field BOLD fMRI mapping of somatosensory cortices in anesthetized monkeys. The stability and reproducibility of the BOLD responses and maps generated from them over periods of up to 20 months confirm the utility of serial non-invasive high field BOLD fMRI mapping sessions for quantifying changes in patterns of cortical activation over long periods time, and this study provides baseline measures for the design of future studies on the plasticity of somatotopic activation following experimental manipulations (behavioral training or spinal cord lesion) in this experimental model.

Stability of BOLD fMRI activation maps of digit in somatosensory area 3b

In adults, the body surface map in primary somatosensory area 3b is generally stable, but can undergo plastic changes (increase, decreased or reorganized cortical territories) in response to behavioral training, injury, or loss of inputs (Pons et al., 1988; Fox et al., 2000; Rosso et al., 2003; Schaefer et al., 2004; Feldman and Brecht, 2005), reviews see (Kaas, 1991; Jones, 2000; Kaas et al., 2007). The functional significance of these plastic changes has been linked to behavioral adaptation and compensation, as well as being a key component of functional recovery (Ungerleider et al., 2002; Godde et al., 2003; Feldman and Brecht, 2005; Schaechter et al., 2006). A complete understanding of the functional relationship between plastic changes in the central nervous system and functional or behavioral outcomes is crucial for developing effective therapeutic interventions. This relationship is not well understood, however, particularly in the primate somatosensory system, due in large part to the difficulty of systematically monitoring and assessing functional reorganization of large areas at multiple

time points over long periods of time following controlled manipulations (e.g. focal spinal cord lesion). Noninvasive high-resolution fMRI is well suited for this purpose. When compared with other high resolution mapping techniques it has the advantages that it can map changes in the larger distributed networks (e.g. SI, SII, and thalamus) involved in somesthesis, and also probe individual network elements (e.g. at the columnar scale) with submillimeter spatial resolution. Once established, the findings can be directly related to human spinal cord injury patients using the same fMRI method.

With that goal in mind, this study aimed to first establish the long-term (weeks to months) baseline intra-subject stability of single condition fMRI activation maps of individual digits, and evaluate the inter-subject variations of digit somatotopy in the primary somatosensory cortex area 3b of primates. In this study we have used single condition (stimulus vs. no stimulus) maps to assess reproducibility and stability of the single digit representations, since it is this that will limit our ability to detect changes in the activation map associated with remodeling of cortical inputs. An commonly used alternative mapping approach (Grinvald et al., 1986; Grinvald et al., 1991; Chen et al., 2005; Duncan and Boynton, 2007), is to generate differential contrast maps, which identify those areas that differ in their response between two stimulus conditions (e.g. D2 vs. D3). However these differential contrasts are not well suited to map the underlying spatial profile of responsiveness to either of the individual stimuli, or to changes in this profile resulting from remodeling of inputs.

We chose to study area 3b in this longitudinal high-resolution fMRI mapping study for several reasons. First, this cortical area has been fairly well characterized, with tight sub-millimeter spatial correlation between electrophysiologically and histologically defined representations for individual digits, linking the functional single digit representations to underlying cytoarchitectural features (Favorov et al., 1987; Pons et al., 1987; Garraghty et al., 1989; Chen et al., 2001; DiCarlo and Johnson, 2002; Sripati et al., 2006). These patches are ~1 mm in diameter, and are well differentiated from each other and from their surroundings (Nelson et al., 1980; Sur et al., 1981; Sur et al., 1982; Pons et al., 1987). Secondly, during stimulation of single distal fingerpads in anesthetized squirrel monkeys, OIS mapping of area 3b at ~50 μm spatial resolution also reveals focal, distinct, millimeter sized activations with limited overlap (~10 %) between adjacent digits (Chen et al., 2001; Chen et al., 2003, , 2009). Finally, the homologous area in human SI with comparable somatotopic organization has also been identified with BOLD fMRI (Nelson and Chen, 2008; Schweizer et al., 2008). In supporting these previous findings, we have shown that at 9.4T, GE-BOLD fMRI can reliably localize and distinguish individual digit activations in single condition maps (Chen et al., 2007), and that with appropriate statistical thresholding (discussed further below), the somatotopic maps of digits generated from single condition maps using the GE-BOLD signal were similar to maps obtained using OIS in the same animal (Chen et al., 2005; Chen et al., 2007). Similar agreement between OIS and GE-BOLD has also be reported in visual cortex (Moon et al., 2007). Extending these findings, this study demonstrated that high-resolution BOLD fMRI could be used to reliably monitor and quantitatively assess the spatial and temporal characteristics of functional digit representations in area 3b. Vibrotactile evoked digit activation in area 3b was quite stable over periods of up to 20 months with ~0.5 mm variability in mapped center across sessions, corresponding to roughly a one half digit representation shift. This half a millimeter variation sets the spatial limit, using the current acquisition protocol, for detecting plastic changes in cortex in our current experimental model system. Interestingly, the variation in digit somatopic maps between individual animals was greater than could be explained by the variations observed within animals across sessions, indicating that the present methods are capable of distinguishing inter-subject variability in somatotopic organization. Given the spatial resolution and sensitivity of the present study, this finding was expected and is consistent with the results obtained with mapping tools such as ultra-high resolution optical imaging at ~ 50 μm resolution (Chen et al., 2005), 2-DG (2-deoxyglucose) (Juliano and

Whitsel, 1985), and electrophysiology mapping studies (Merzenich et al., 1987). This inter-subject variation in digit baseline somatotopy, as well as the wide variability in the nature and degree of reorganization likely across individuals (Kaas, 1991; Jones, 2000; Kaas et al., 2007), underscores the importance of the ability to monitor and assess plastic changes at the individual subject level.

The magnitude and temporal profile of BOLD signals across imaging sessions was also quite stable, and the mean BOLD signal change (~ 0.6%) was consistent with previous studies at 9.4T by ourselves (Chen et al., 2007) and others (Kim et al., 2000; Cohen et al., 2002). This study extends these previous reports by quantifying, for the first time, the long-term spatial, temporal and signal amplitude stability of single digit representation maps in area 3b obtained using the BOLD mapping signal. Knowledge of the limits of long term (weeks to months) intra-subject reproducibility of BOLD activation maps in normal subjects is an essential prerequisite for defining the sensitivity with which dynamic functional changes in the central nervous system, whether in response to injury, deafferentation, or rehabilitation, can be observed. In this regard, the reproducibility and stability of maps obtained using GE-BOLD are of particular interest, given its wide adoption in human brain mapping studies.

Factors contributing to the stability of high field BOLD fMRI maps

Several technical and biological factors may influence the run to run and session to session reproducibility and stability of these BOLD maps. These include variation in image slice positioning, accuracy of image co-registration algorithms, image acquisition point spread functions (Shmuel et al., 2007), contrast to noise ratio of the BOLD signal, stability and reproducibility of the stimulus and the animal's physiological state across imaging sessions (Dagli et al., 1999; Peeters et al., 2001; Kannurpatti et al., 2003; Zhang et al., 2007; Goense and Logothetis, 2008).

In a high-resolution fMRI experiment, typically, whole brain coverage is traded for high spatial resolution with partial brain volume coverage. Variability in planning of imaging planes across imaging sessions could be a significant contributor to the stability of activations to be monitored. Depending on the region of interest, a range of approaches may be used to guide image slice positioning. In this study, anatomical and fine vascular landmarks were used both for positioning of imaging slices and also for subsequent across session image coregistration. High resolution T2* weighted images visualized the network of pial and even small trans-cortical veins, providing a rich set of landmarks for guiding slice planning and coregistration with sub-voxel accuracy (Fitzpatrick and West, 2001). The sub-millimeter reproducibility of the locations of digit activation centers across runs within a session observed in the present study is comparable to published studies at ultra high field (Fukuda et al., 2006; Schafer et al., 2006; Moon et al., 2007). This spatial variability is close to that of the native resolution at which the functional maps were collected. Theoretically, the stability (or reproducibility) of single digit maps can be improved by increasing spatial imaging resolution, provided that the BOLD contrast to noise is not degraded significantly by the reduced voxel dimensions (Fukuda et al., 2006; Shmuel et al., 2007).

It is generally observed that draining veins contribute significantly to the fMRI maps collected using GE-BOLD fMRI at lower field strengths, limiting the available spatial resolution, particularly when compared with spin-echo BOLD mapping. We believe that at least two biophysical factors may contribute to our ability to obtain GE-BOLD maps with sub-millimeter reproducibility in this study. First, the shorter T2 of the intravascular signal (~9 ms vs ~40 ms for tissue, (Lee et al., 1999)) greatly reduces the contribution of intravascular water, and accentuates the contribution of extravascular BOLD signals. These effects are already evident at 7T compared with 3T and 1.5T, where intravascular draining veins may dominate the BOLD PSF (Menon and Goodyear, 1999; Shmuel et al., 2007). Taken together, high MRI field

provides significant benefits for signal specificity. Second, it is likely that the mild and focal physiological activation of a single fingertip representation in area 3b has relatively little effect on the deoxyhemoglobin concentration in even relatively small draining venules and veins, reducing their contribution to extravascular BOLD effects and consequently their influence on the BOLD PSF (point spread function). Such an explanation is consistent with recent studies by Moon and colleagues (Moon et al., 2007) who have demonstrated that while the PSF of the GE-BOLD mapping signal in cat primary visual cortex at 9.4T is roughly twice that of the SE-BOLD PSF, it is nonetheless possible to resolve a spacing of 1.4 ± 0.05 mm between iso-orientation patches using GE-BOLD mapping, and agreement to ~0.22 mm, between iso-orientation domains mapped using SE-BOLD and OIS as the mapping signal, considerably less than the dimensions of individual cortical columns. Physiologically, it is well known that the BOLD signal is sensitive to the type and level of anesthesia (Peeters et al., 2001; Kannurpatti and Biswal, 2004; Goense and Logothetis, 2008), pCO2 ((Landuyt et al., 2001; Cohen et al., 2002; Kannurpatti et al., 2003; Macey et al., 2004; Thomason et al., 2005) and BP (Harper et al., 1998; Wang et al., 2006). Therefore, continuous monitoring and tight control of physiology (ETCO2, HR, temp, anesthesia level) of animal condition during imaging is essential.

Mapping cortical function longitudinally

Error associated with misregistration of functional maps collected across imaging sessions contributes to the spatial variance in longitudinal studies. Co-registration errors are likely to be low for maps generated within a single imaging session in anesthetized, stereotaxically immobilized animals, but are a probable contributor to the increased variation in location of activation peaks across sessions, compared with within sessions, particularly for high resolution studies. Nonetheless, this inter-session variability contributed only a small additional 0.14 mm error (mean pairwise distance between centers of activation across all runs for a single digit was 0.55 ± 0.15 across sessions compared with 0.41 ± 0.24 mm (mean ± SD) within sessions), despite the fact that in this study the coregistration algorithm corrected only in-plane misregistration, using manually identified structural and vascular landmarks, and did not correct for any misregistration of slice location and or slice angulation between sessions (Fitzpatrick and West, 2001; West et al., 2001). Thus, with improved full 3D coregistration we anticipate that inter-session coregistration error may be further reduced. In sum, our data demonstrated that BOLD fMRI with our current imaging acquisition and co-registration settings is capable of detecting submillimeter changes in functional representations over periods of weeks to many months in a non-invasive manner that is ideally suited for longitudinal studies of functional reorganization and plasticity of the primate brain.

Measurements for assessing spatio-temporal stability of GE-BOLD mapping signal

We have examined a range of measures of intra-subject inter-session reproducibility of GE-BOLD activation maps, including the center of mass of activation (Rombouts et al., 1998), average signal amplitude (Rombouts et al., 1998; van Gelderen et al., 2005; Leontiev and Buxton, 2007), normalized statistical threshold (Waldvogel et al., 2000; Yoo et al., 2005; Harrington et al., 2006), and the temporal profile of the BOLD signal (Neumann et al., 2003). Of these, and consistent with previous studies (Rombouts et al., 1998; van Gelderen et al., 2005), we found the center of activation and average signal amplitude to be the most stable measurements for assessing intra-subject reproducibility of BOLD activation maps. Indeed our current study confirmed that the location of GE-BOLD activation centers, signal amplitudes and temporal profiles of individual digit response in somatosensory area 3b were reproducible over periods of up to 20 months. As we have established in a previous paper (Chen et al., 2007) and in this study, changing the statistical threshold of the fMRI maps led to various degrees of changes in the estimated area of activation, but did not alter the location. However, one caveat is that the activation size and boundaries varied the most across sessions even when different statistical threshold criteria were used. Importantly, the variation in BOLD activation

size is significantly larger than what we have observed with optical imaging method. This finding is not surprisingly given the significant imaging resolution differences (50 μm in OIs versus 625 μm in fMRI), and differences in image analytic approaches generally employed (Chen et al., 2007). In addition, given the already known differences in origins of mapping signals, one should be cautious in the interpretation of spatial map differences (e.g. size, location and shape) as revealed by different mapping methods such as fMRI, OIS, receptive field mapping. Differences in contributions from neural activity, neurovascular coupling, and/or hemodynamic component of mapping signal may all contribute to the map differences. Further studies focusing on understanding of spatial correlations between various components of mapping signal are urgently needed.

In sum, these observations suggest that the locations of the strongest BOLD activation, irrespective of threshold, rather than the size of activation determined by various criteria may be a more stable measurement for monitoring cortical functional organization longitudinally particularly in anesthetized animals. This study provides baseline measures of the variation of high-resolution BOLD fMRI for future long-term intra-subject applications assessing brain plasticity at millimeter scales.

5. Conclusions

In this paper, we have quantified the intra-subject variation of single digit BOLD activation maps generated using vibrotactile stimulation, and examined the inter-subject variation of these digit somatopy maps. Our data confirm that GE-BOLD fMRI can be used to reproducibly map fine scale functional organization longitudinally with sub-millimeter resolution. The observed inter-subject variability in digit somatotopy underscores the importance of mapping fine scale functional maps longitudinally in individual subjects when assessing fine functional reorganization, and suggests that such reorganization can be tracked with submillimeter sensitivity using current GE-BOLD fMRI methodologies.

Acknowledgments

National of Health Grants DA024831 (LMC), DE16606 (LMC), DA028303 (MJA), EB000461 (JCG), EB002326 (JCG), and Vanderbilt University Medical Center Discovery Grant (MJA) supported this work. We thank Dr. Robert Friedman for his comments on manuscript and Chaohui Tang for technique support on fMRI data collection.

References

Chen LM, Friedman RM, Roe AW. Optical imaging of a tactile illusion in area 3b of the primary somatosensory cortex. Science 2003;302:881–885. [PubMed: 14500850]

Chen LM, Friedman RM, Roe AW. Optical imaging of SI topography in anesthetized and awake squirrel monkeys. J Neurosci 2005;25:7648–7659. [PubMed: 16107651]

Chen LM, Friedman RM, Roe AW. Optical imaging of digit topography in individual awake and anesthetized squirrel monkeys. Exp Brain Res 2009;196:393–401. [PubMed: 19484466]

Chen LM, Friedman RM, Ramsden BM, LaMotte RH, Roe AW. Fine-scale organization of SI (area 3b) in the squirrel monkey revealed with intrinsic optical imaging. J Neurophysiol 2001;86:3011–3029. [PubMed: 11731557]

Chen LM, Heider B, Williams GV, Healy FL, Ramsden BM, Roe AW. A chamber and artificial dura method for long-term optical imaging in the monkey. J Neurosci Methods 2002;113:41–49. [PubMed: 11741720]

Chen LM, Turner GH, Friedman RM, Zhang N, Gore JC, Roe AW, Avison MJ. High-resolution maps of real and illusory tactile activation in primary somatosensory cortex in individual monkeys with functional magnetic resonance imaging and optical imaging. J Neurosci 2007;27:9181–9191. [PubMed: 17715354]

Cohen ER, Ugurbil K, Kim SG. Effect of basal conditions on the magnitude and dynamics of the blood oxygenation level-dependent fMRI response. J Cereb Blood Flow Metab 2002;22:1042–1053. [PubMed: 12218410]

Costafreda SG, Brammer MJ, Vencio RZ, Mourao ML, Portela LA, de Castro CC, Giampietro VP, Amaro E Jr. Multisite fMRI reproducibility of a motor task using identical MR systems. J Magn Reson Imaging 2007;26:1122–1126. [PubMed: 17896376]

Courtine G, Bunge MB, Fawcett JW, Grossman RG, Kaas JH, Lemon R, Maier I, Martin J, Nudo RJ, Ramon-Cueto A, Rouiller EM, Schnell L, Wannier T, Schwab ME, Edgerton VR. Can experiments in nonhuman primates expedite the translation of treatments for spinal cord injury in humans? Nat Med 2007;13:561–566. [PubMed: 17479102]

Dagli MS, Ingeholm JE, Haxby JV. Localization of cardiac-induced signal change in fMRI. Neuroimage 1999;9:407–415. [PubMed: 10191169]

DiCarlo JJ, Johnson KO. Receptive field structure in cortical area 3b of the alert monkey. Behav Brain Res 2002;135:167–178. [PubMed: 12356447]

Disbrow E, Roberts TP, Slutsky D, Krubitzer L. The use of fMRI for determining the topographic organization of cortical fields in human and nonhuman primates. Brain Res 1999;829:167–173. [PubMed: 10350543]

Disbrow EA, Slutsky DA, Roberts TP, Krubitzer LA. Functional MRI at 1.5 tesla: a comparison of the blood oxygenation level-dependent signal and electrophysiology. Proc Natl Acad Sci U S A 2000;97:9718–9723. [PubMed: 10931954]

Duncan RO, Boynton GM. Tactile hyperacuity thresholds correlate with finger maps in primary somatosensory cortex (S1). Cereb Cortex 2007;17:2878–2891. [PubMed: 17372277]

Favorov O, Whitsel BL. Spatial organization of the peripheral input to area 1 cell columns. II. The forelimb representation achieved by a mosaic of segregates. Brain Res 1988a;472:43–56. [PubMed: 3342335]

Favorov O, Whitsel BL. Spatial organization of the peripheral input to area 1 cell columns. I. The detection of ‘segregates’. Brain Res 1988b;472:25–42. [PubMed: 3342334]

Favorov OV, Diamond ME, Whitsel BL. Evidence for a mosaic representation of the body surface in area 3b of the somatic cortex of cat. Proc Natl Acad Sci U S A 1987;84:6606–6610. [PubMed: 3476963]

Feldman DE, Brecht M. Map plasticity in somatosensory cortex. Science 2005;310:810–815. [PubMed: 16272113]

Fernandez G, Specht K, Weis S, Tendolkar I, Reuber M, Fell J, Klaver P, Ruhlmann J, Reul J, Elger CE. Intrasubject reproducibility of presurgical language lateralization and mapping using fMRI. Neurology 2003;60:969–975. [PubMed: 12654961]

Fitzpatrick JM, West JB. The distribution of target registration error in rigid-body point-based registration. IEEE Trans Med Imaging 2001;20:917–927. [PubMed: 11585208]

Fox K, Glazewski S, Schulze S. Plasticity and stability of somatosensory maps in thalamus and cortex. Curr Opin Neurobiol 2000;10:494–497. [PubMed: 10981619]

Friedman RM, Chen LM, Roe AW. Modality maps within primate somatosensory cortex. Proc Natl Acad Sci U S A 2004;101:12724–12729. [PubMed: 15308779]

Friedman RM, Chen LM, Roe AW. Responses of areas 3b and 1 in anesthetized squirrel monkeys to single and dual site stimulation of the digits. J Neurophysiol. 2008

Fukuda M, Moon CH, Wang P, Kim SG. Mapping iso-orientation columns by contrast agent-enhanced functional magnetic resonance imaging: reproducibility, specificity, and evaluation by optical imaging of intrinsic signal. J Neurosci 2006;26:11821–11832. [PubMed: 17108155]

Fukuda M, Rajagopalan UM, Homma R, Matsumoto M, Nishizaki M, Tanifuji M. Localization of activity-dependent changes in blood volume to submillimeter-scale functional domains in cat visual cortex. Cereb Cortex 2005;15:823–833. [PubMed: 15459078]

Garraghty PE, Pons TP, Sur M, Kaas JH. The arbors of axons terminating in middle cortical layers of somatosensory area 3b in owl monkeys. Somatosens Mot Res 1989;6:401–411. [PubMed: 2756803]

Gelnar PA, Krauss BR, Szeverenyi NM, Apkarian AV. Fingertip representation in the human somatosensory cortex: an fMRI study. Neuroimage 1998;7:261–283. [PubMed: 9626668]

Godde B, Ehrhardt J, Braun C. Behavioral significance of input-dependent plasticity of human somatosensory cortex. Neuroreport 2003;14:543–546. [PubMed: 12657881]

Goense JB, Logothetis NK. Neurophysiology of the BOLD fMRI signal in awake monkeys. Curr Biol 2008;18:631–640. [PubMed: 18439825]

Grinvald A, Frostig RD, Siegel RM, Bartfeld E. High-resolution optical imaging of functional brain architecture in the awake monkey. Proc Natl Acad Sci U S A 1991;88:11559–11563. [PubMed: 1763070]

Grinvald A, Lieke E, Frostig RD, Gilbert CD, Wiesel TN. Functional architecture of cortex revealed by optical imaging of intrinsic signals. Nature 1986;324:361–364. [PubMed: 3785405]

Harper RM, Gozal D, Bandler R, Spriggs D, Lee J, Alger J. Regional brain activation in humans during respiratory and blood pressure challenges. Clin Exp Pharmacol Physiol 1998;25:483–486. [PubMed: 9673830]

Harrington GS, Tomaszewski Farias S, Buonocore MH, Yonelinas AP. The intersubject and intrasubject reproducibility of FMRI activation during three encoding tasks: implications for clinical applications. Neuroradiology 2006;48:495–505. [PubMed: 16703360]

Hill DL, Hawkes DJ, Crossman JE, Gleeson MJ, Cox TC, Bracey EE, Strong AJ, Graves P. Registration of MR and CT images for skull base surgery using point-like anatomical features. Br J Radiol 1991;64:1030–1035. [PubMed: 1742584]

Jones EG. Cortical and subcortical contributions to activity-dependent plasticity in primate somatosensory cortex. Annu Rev Neurosci 2000;23:1–37. [PubMed: 10845057]

Juliano SL, Whitsel BL. Metabolic labeling associated with index finger stimulation in monkey SI: between animal variability. Brain Res 1985;342:242–251. [PubMed: 4041824]

Kaas JH. Plasticity of sensory and motor maps in adult mammals. Annu Rev Neurosci 1991;14:137–167. [PubMed: 2031570]

Kaas JH. The reorganization of somatosensory and motor cortex after peripheral nerve or spinal cord injury in primates. Prog Brain Res 2000;128:173–179. [PubMed: 11105677]

Kaas JH, Qi HX, Burish MJ, Gharbawie OA, Onifer SM, Massey JM. Cortical and subcortical plasticity in the brains of humans, primates, and rats after damage to sensory afferents in the dorsal columns of the spinal cord. Exp Neurol. 2007

Kannurpatti SS, Biswal BB. Effect of anesthesia on CBF, MAP and fMRI-BOLD signal in response to apnea. Brain Res 2004;1011:141–147. [PubMed: 15157800]

Kannurpatti SS, Biswal BB, Hudetz AG. Baseline physiological state and the fMRI-BOLD signal response to apnea in anesthetized rats. NMR Biomed 2003;16:261–268. [PubMed: 14648886]

Kida I, Xu F, Shulman RG, Hyder F. Mapping at glomerular resolution: fMRI of rat olfactory bulb. Magn Reson Med 2002;48:570–576. [PubMed: 12210928]

Kim DS, Duong TQ, Kim SG. High-resolution mapping of iso-orientation columns by fMRI. Nat Neurosci 2000;3:164–169. [PubMed: 10649572]

Kohn A, Pinheiro A, Tommerdahl MA, Whitsel BL. Optical imaging in vitro provides evidence for the minicolumnar nature of cortical response. Neuroreport 1997;8:3513–3518. [PubMed: 9427317]

Krause T, Kurth R, Ruben J, Schwiemann J, Villringer K, Deuchert M, Moosmann M, Brandt S, Wolf K, Curio G, Villringer A. Representational overlap of adjacent fingers in multiple areas of human primary somatosensory cortex depends on electrical stimulus intensity: an fMRI study. Brain Res 2001;899:36–46. [PubMed: 11311865]

Landuyt W, Hermans R, Bosmans H, Sunaert S, Beatse E, Farina D, Meijerink M, Zhang H, Van Den Bogaert W, Lambin P, Marchal G. BOLD contrast fMRI of whole rodent tumour during air or carbogen breathing using echo-planar imaging at 1.5 T. Eur Radiol 2001;11:2332–2340. [PubMed: 11702181]

Lauritzen M, Gold L. Brain function and neurophysiological correlates of signals used in functional neuroimaging. J Neurosci 2003;23:3972–3980. [PubMed: 12764081]

Lee SP, Silva AC, Ugurbil K, Kim SG. Diffusion-weighted spin-echo fMRI at 9.4 T: microvascular/tissue contribution to BOLD signal changes. Magn Reson Med 1999;42:919–928. [PubMed: 10542351]

Leontiev O, Buxton RB. Reproducibility of BOLD, perfusion, and CMRO2 measurements with calibrated-BOLD fMRI. Neuroimage 2007;35:175–184. [PubMed: 17208013]

Logothetis NK, Pauls J, Augath M, Trinath T, Oeltermann A. Neurophysiological investigation of the basis of the fMRI signal. Nature 2001;412:150–157. [PubMed: 11449264]

Macey KE, Macey PM, Woo MA, Harper RK, Alger JR, Keens TG, Harper RM. fMRI signal changes in response to forced expiratory loading in congenital central hypoventilation syndrome. J Appl Physiol 2004;97:1897–1907. [PubMed: 15258126]

Maldjian JA, Gottschalk A, Patel RS, Detre JA, Alsop DC. The sensory somatotopic map of the human hand demonstrated at 4 Tesla. Neuroimage 1999;10:55–62. [PubMed: 10385581]

Meier JD, Aflalo TN, Kastner S, Graziano MS. Complex organization of human primary motor cortex: a high-resolution fMRI study. J Neurophysiol 2008;100:1800–1812. [PubMed: 18684903]

Menon RS, Goodyear BG. Submillimeter functional localization in human striate cortex using BOLD contrast at 4 Tesla: implications for the vascular point-spread function. Magn Reson Med 1999;41:230–235. [PubMed: 10080267]

Menz MM, Neumann J, Muller K, Zysset S. Variability of the BOLD response over time: an examination of within-session differences. Neuroimage 2006;32:1185–1194. [PubMed: 16857390]

Merzenich MM, Nelson RJ, Kaas JH, Stryker MP, Jenkins WM, Zook JM, Cynader MS, Schoppmann A. Variability in hand surface representations in areas 3b and 1 in adult owl and squirrel monkeys. J Comp Neurol 1987;258:281–296. [PubMed: 3584541]

Moon CH, Fukuda M, Park SH, Kim SG. Neural interpretation of blood oxygenation level-dependent fMRI maps at submillimeter columnar resolution. J Neurosci 2007;27:6892–6902. [PubMed: 17596437]

Moser E, Teichtmeister C, Diemling M. Reproducibility and postprocessing of gradient-echo functional MRI to improve localization of brain activity in the human visual cortex. Magn Reson Imaging 1996;14:567–579. [PubMed: 8897359]

Mountcastle VB. Modality and topographic properties of single neurons of cat's somatic sensory cortex. J Neurophysiol 1957;20:408–434. [PubMed: 13439410]

Mountcastle VB. The columnar organization of the neocortex. Brain 1997;120 (Pt 4):701–722. [PubMed: 9153131]

Mountcastle VB. Introduction. Computation in cortical columns. Cereb Cortex 2003;13:2–4. [PubMed: 12466209]

Nelson AJ, Chen R. Digit somatotopy within cortical areas of the postcentral gyrus in humans. Cereb Cortex 2008;18:2341–2351. [PubMed: 18245039]

Nelson RJ, Sur M, Felleman DJ, Kaas JH. Representations of the body surface in postcentral parietal cortex of Macaca fascicularis. J Comp Neurol 1980;192:611–643. [PubMed: 7419747]

Neumann J, Lohmann G, Zysset S, von Cramon DY. Within-subject variability of BOLD response dynamics. Neuroimage 2003;19:784–796. [PubMed: 12880807]

Peeters RR, Tindemans I, De Schutter E, Van der Linden A. Comparing BOLD fMRI signal changes in the awake and anesthetized rat during electrical forepaw stimulation. Magn Reson Imaging 2001;19:821–826. [PubMed: 11551722]

Pons TP, Garraghty PE, Mishkin M. Lesion-induced plasticity in the second somatosensory cortex of adult macaques. Proc Natl Acad Sci U S A 1988;85:5279–5281. [PubMed: 3393538]

Pons TP, Wall JT, Garraghty PE, Cusick CG, Kaas JH. Consistent features of the representation of the hand in area 3b of macaque monkeys. Somatosens Res 1987;4:309–331. [PubMed: 3589287]

Reed JL, Pouget P, Qi HX, Zhou Z, Bernard MR, Burish MJ, Haitas J, Bonds AB, Kaas JH. Widespread spatial integration in primary somatosensory cortex. Proc Natl Acad Sci U S A 2008;105:10233–10237. [PubMed: 18632579]

Rombouts SA, Barkhof F, Hoogenraad FG, Sprenger M, Scheltens P. Within-subject reproducibility of visual activation patterns with functional magnetic resonance imaging using multislice echo planar imaging. Magn Reson Imaging 1998;16:105–113. [PubMed: 9508267]

Rosso T, Aglioti SM, Zanette G, Ischia S, Finco G, Farina S, Fiaschi A, Tinazzi M. Functional plasticity in the human primary somatosensory cortex following acute lesion of the anterior lateral spinal cord: neurophysiological evidence of short-term cross-modal plasticity. Pain 2003;101:117–127. [PubMed: 12507706]

Salli E, Korvenoja A, Visa A, Katila T, Aronen HJ. Reproducibility of fMRI: effect of the use of contextual information. Neuroimage 2001;13:459–471. [PubMed: 11170811]

Schaechter JD, Moore CI, Connell BD, Rosen BR, Dijkhuizen RM. Structural and functional plasticity in the somatosensory cortex of chronic stroke patients. Brain 2006;129:2722–2733. [PubMed: 16921177]

Schaefer M, Rothemund Y, Heinze HJ, Rotte M. Short-term plasticity of the primary somatosensory cortex during tool use. Neuroreport 2004;15:1293–1297. [PubMed: 15167552]

Schafer JR, Kida I, Xu F, Rothman DL, Hyder F. Reproducibility of odor maps by fMRI in rodents. Neuroimage 2006;31:1238–1246. [PubMed: 16632382]

Schweizer R, Voit D, Frahm J. Finger representations in human primary somatosensory cortex as revealed by high-resolution functional MRI of tactile stimulation. Neuroimage 2008;42:28–35. [PubMed: 18550386]

Shmuel A, Yacoub E, Chaimow D, Logothetis NK, Ugurbil K. Spatio-temporal point-spread function of fMRI signal in human gray matter at 7 Tesla. Neuroimage 2007;35:539–552. [PubMed: 17306989]

Sripati AP, Yoshioka T, Denchev P, Hsiao SS, Johnson KO. Spatiotemporal receptive fields of peripheral afferents and cortical area 3b and 1 neurons in the primate somatosensory system. J Neurosci 2006;26:2101–2114. [PubMed: 16481443]

Sur M, Wall JT, Kaas JH. Modular segregation of functional cell classes within the postcentral somatosensory cortex of monkeys. Science 1981;212:1059–1061. [PubMed: 7233199]

Sur M, Nelson RJ, Kaas JH. Representations of the body surface in cortical areas 3b and 1 of squirrel monkeys: comparisons with other primates. J Comp Neurol 1982;211:177–192. [PubMed: 7174889]

Sur M, Wall JT, Kaas JH. Modular distribution of neurons with slowly adapting and rapidly adapting responses in area 3b of somatosensory cortex in monkeys. J Neurophysiol 1984;51:724–744. [PubMed: 6716121]

Tegeler C, Strother SC, Anderson JR, Kim SG. Reproducibility of BOLD-based functional MRI obtained at 4 T. Hum Brain Mapp 1999;7:267–283. [PubMed: 10408770]

Thomason ME, Burrows BE, Gabrieli JD, Glover GH. Breath holding reveals differences in fMRI BOLD signal in children and adults. Neuroimage 2005;25:824–837. [PubMed: 15808983]

Tjandra T, Brooks JC, Figueiredo P, Wise R, Matthews PM, Tracey I. Quantitative assessment of the reproducibility of functional activation measured with BOLD and MR perfusion imaging: implications for clinical trial design. Neuroimage 2005;27:393–401. [PubMed: 15921936]

Tommerdahl M, Favorov O, Whitsel BL. Optical imaging of intrinsic signals in somatosensory cortex. Behav Brain Res 2002;135:83–91. [PubMed: 12356438]

Tommerdahl M, Delemos KA, Whitsel BL, Favorov OV, Metz CB. Response of anterior parietal cortex to cutaneous flutter versus vibration. J Neurophysiol 1999;82:16–33. [PubMed: 10400931]

Ungerleider LG, Doyon J, Karni A. Imaging brain plasticity during motor skill learning. Neurobiol Learn Mem 2002;78:553–564. [PubMed: 12559834]

van Gelderen P, C WHW, de Zwart JA, Cohen L, Hallett M, Duyn JH. Resolution and reproducibility of BOLD and perfusion functional MRI at 3.0 Tesla. Magn Reson Med 2005;54:569–576. [PubMed: 16086372]

Vanzetta I, Grinvald A. Coupling between neuronal activity and microcirculation: implications for functional brain imaging. Hfsp J 2008;2:79–98. [PubMed: 19404475]

Waldvogel D, van Gelderen P, Immisch I, Pfeiffer C, Hallett M. The variability of serial fMRI data: correlation between a visual and a motor task. Neuroreport 2000;11:3843–3847. [PubMed: 11117501]

Wang R, Foniok T, Wamsteeker JI, Qiao M, Tomanek B, Vivanco RA, Tuor UI. Transient blood pressure changes affect the functional magnetic resonance imaging detection of cerebral activation. Neuroimage 2006;31:1–11. [PubMed: 16460967]

West JB, Fitzpatrick JM, Toms SA, Maurer CR Jr, Maciunas RJ. Fiducial point placement and the accuracy of point-based, rigid body registration. Neurosurgery 2001;48:810–816. [PubMed: 11322441]discussion 816–817

Whalley HC, Gountouna VE, Hall J, McIntosh AM, Simonotto E, Job DE, Owens DG, Johnstone EC, Lawrie SM. fMRI changes over time and reproducibility in unmedicated subjects at high genetic risk of schizophrenia. Psychol Med 2009;39:1189–1199. [PubMed: 19105855]

Yacoub E, Harel N, Ugurbil K. High-field fMRI unveils orientation columns in humans. Proc Natl Acad Sci U S A 2008;105:10607–10612. [PubMed: 18641121]

Yang X, Hyder F, Shulman RG. Functional MRI BOLD signal coincides with electrical activity in the rat whisker barrels. Magn Reson Med 1997;38:874–877. [PubMed: 9402186]

Yoo SS, Wei X, Dickey CC, Guttmann CR, Panych LP. Long-term reproducibility analysis of fMRI using hand motor task. Int J Neurosci 2005;115:55–77. [PubMed: 15768852]

Yoo SS, O'Leary HM, Lee JH, Chen NK, Panych LP, Jolesz FA. Reproducibility of trial-based functional MRI on motor imagery. Int J Neurosci 2007;117:215–227. [PubMed: 17365109]

Zhang N, Gore JC, Chen LM, Avison MJ. Dependence of BOLD signal change on tactile stimulus intensity in SI of primates. Magn Reson Imaging 2007;25:784–794. [PubMed: 17614230]

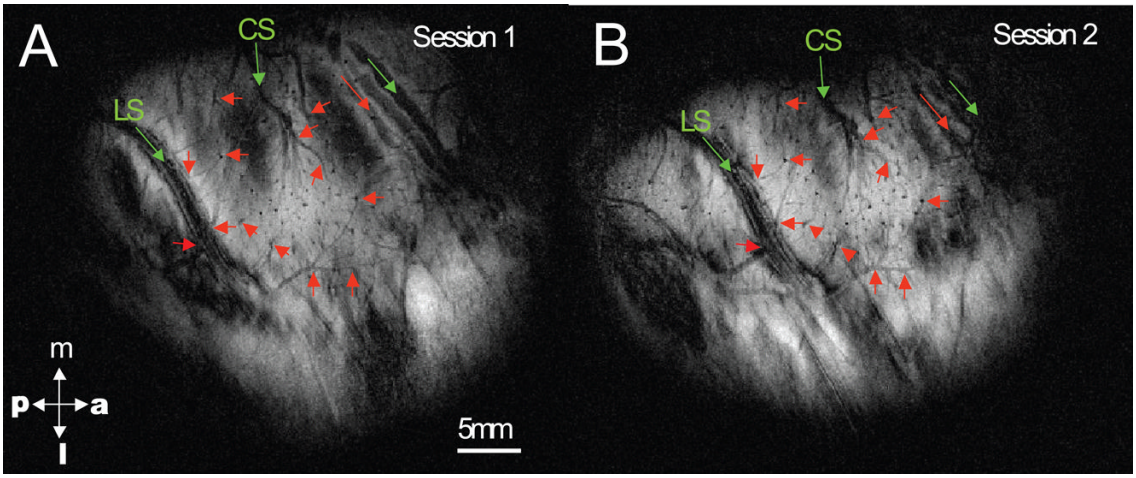

Figure 1.

Across session image alignment. Two T2* weighted structural images (A: session 1; B: session 2) were aligned based on the local structural and blood vessel landmarks around area 3b area. Color arrows indicated the selected landmarks used for co-registration. Red arrows: small venous structures; green arrows: large veins and sulci. CS: central sulcus. LS: lateral sulcus. m: middle. p: posterior. a: anterior. l: lateral.

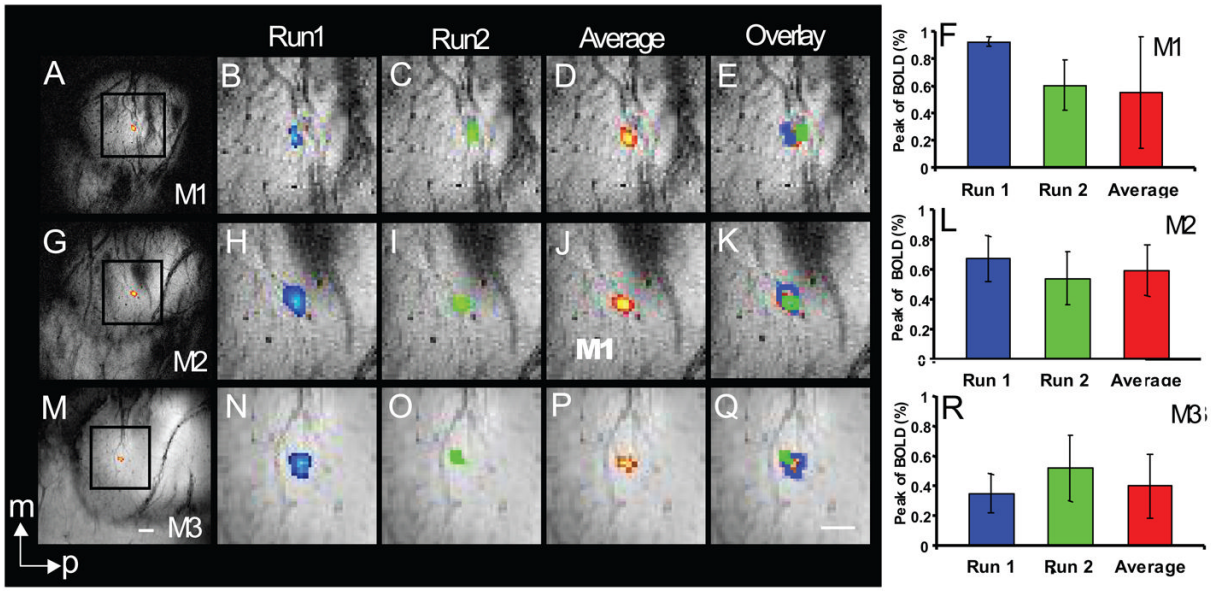

Figure 2.

Within session reproducibility of BOLD activation centers and percentage BOLD signal change in three monkeys (M1–M3). A–F: M1 with D4 stimulation; G–L: M2 with D4 stimulation; M–R: M3 with D3 stimulation). Single-condition single digit activation maps from two runs were compared in each individual monkey (M1–M3; blue activations for run 1, green activations for run 2). The averaged activation maps (see method) across two runs are shown in D, J and P for M1, M2 and M3, respectively. E, K, Q show the composite outlines of the single session activations (green and blue outlines) over the averaged activation map (yellow-red patches). The actual statistical significance values (p) identified in run1, run2 and average run in each animal are $p<10^{-5}$, 10^{-14} and 10^{-10} in M1, $p<10^{-4}$, 10^{-7} and 10^{-9} in M2, and $p<10^{-12}$, 10^{-12} and 10^{-12} in M3. F, L, and R: maximum BOLD signal (± SD) amplitudes across runs (blue and green columns) and in average (red columns) in M1–M3 monkeys. White scale bars indicate 1mm scale. m: medial; a: anterior.

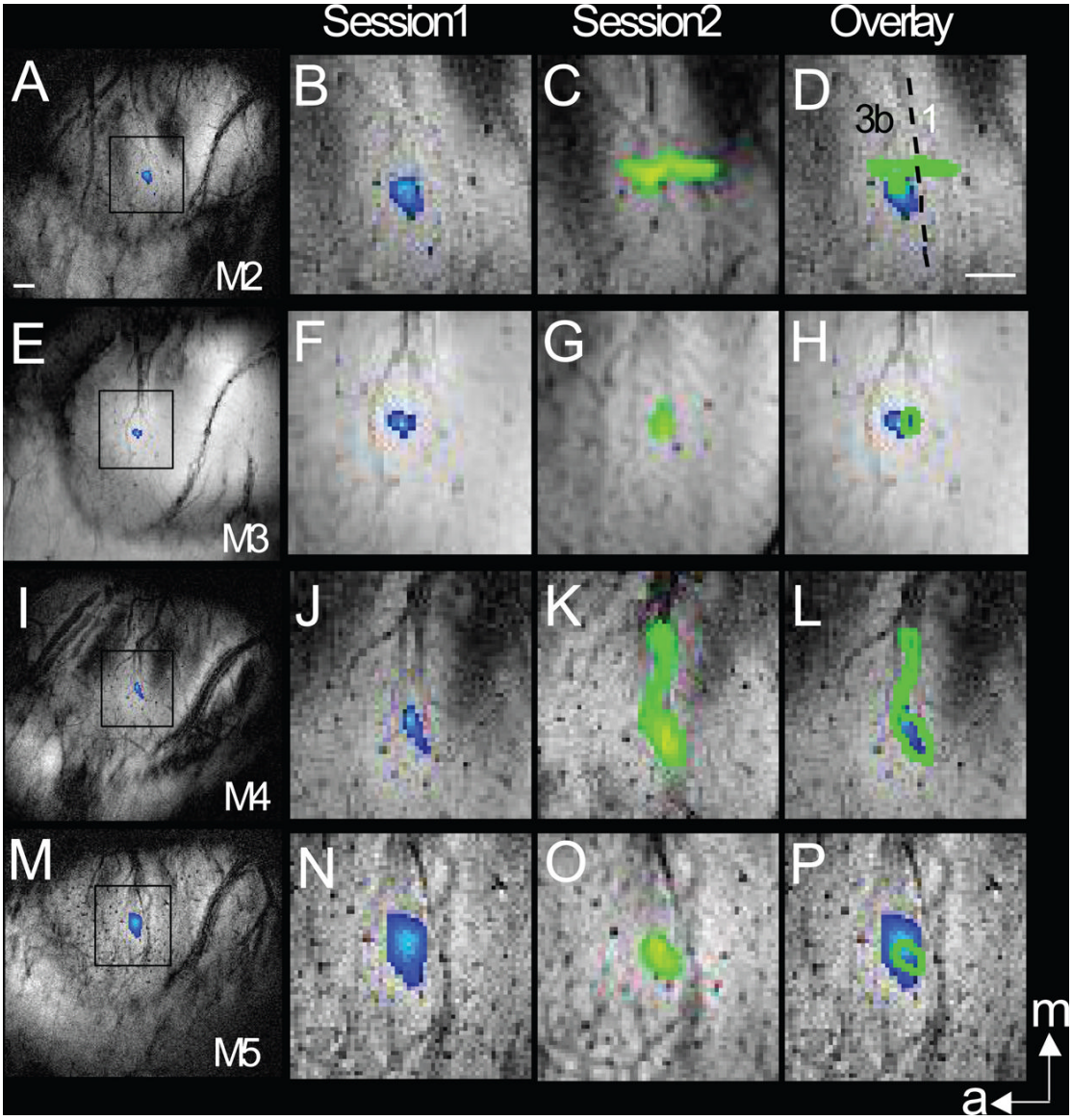

Figure 3.

Cross-session reproducibility of the BOLD activation location in monkeys M2, M3, M4, M5. Single condition activation maps of individual finger pad acquired on separate sessions (blue patches for session 1, green patches for session 2) for each animal are shown. A–C: M1 with D3 stimulation; E–G M2 with D3 stimulation; I–K: M3 with D3 stimulation; M–O: M4 with D3 stimulation. Session 1 and session 2 images were co-registered (see method), overlaid and shown in D, H, L, P, using green outlines to indicate the session 1 activation. The p thresholds ($10^2 \times p_{min}$) for each animal are M1: $p<10^{-9}$ session 1 (A, B), $p<10^{-5}$ session 2 (C); M2: $p<10^{-14}$ session 1 (E, F), $p<10^{-5}$ on session 2 (G); M3: $p< 10^{-12}$ session 1 (I, J), $p<10^{-14}$ (K) session 2.; M4: $p< 10^{-14}$ session 1 (M, N), $p<10^{-14}$ session 2 (O). White scale bars indicate 1mm scale. m: medial; a: anterior.

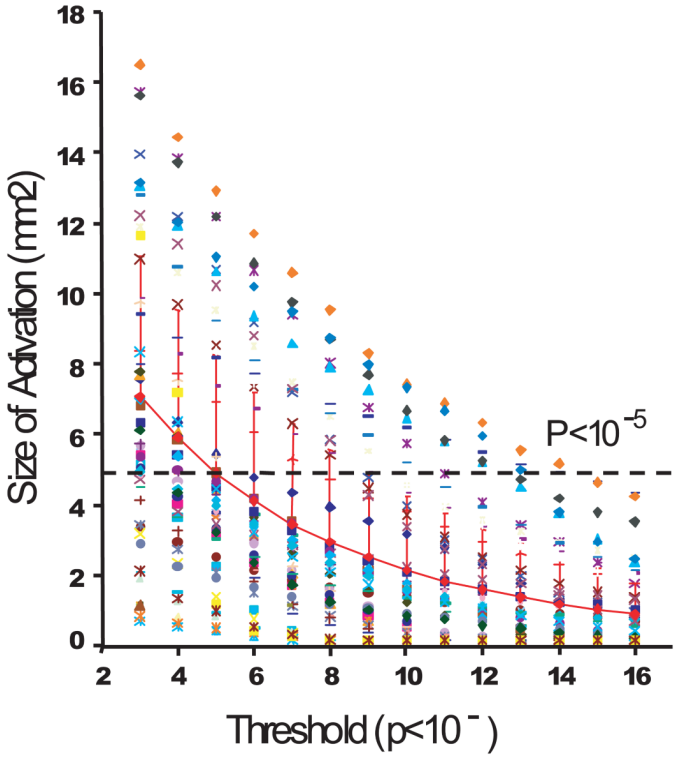

Figure 4.

Relationship between statistical threshold and size of activation in area 3b. Sizes of activation in mm2 are plotted as a functional of statistical threshold (p values) for each imaging run across all imaging sessions (total of 49 runs). Thresholds range from 10^{-3} to 10^{-16}. Each symbol represents measures from one run. Red diamond line with error bars indicates the mean size of activation plus standard deviation. Black dotted line indicates the mean size of activation along y-axis when the threshold is set at $p<10^{-5}$.

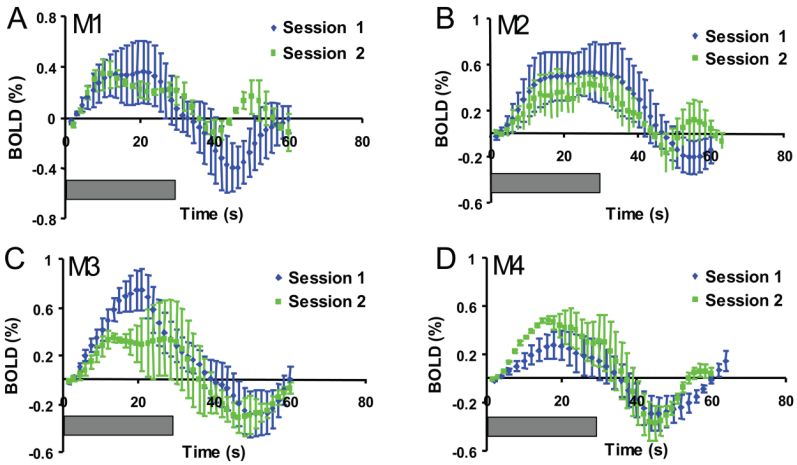

Figure 5.

Comparison of BOLD signal temporal profiles across image sessions. Temporal profiles of averaged multiple trial BOLD signal changes in area 3b for M1 – M4 (Session 1: blue curves; Session 2: green curves). Each point on the curve represented the mean ± SD signal amplitude measured from a common region of interest for each animal. Grey bars indicate the 30 sec duration of vibrotactile stimulation.

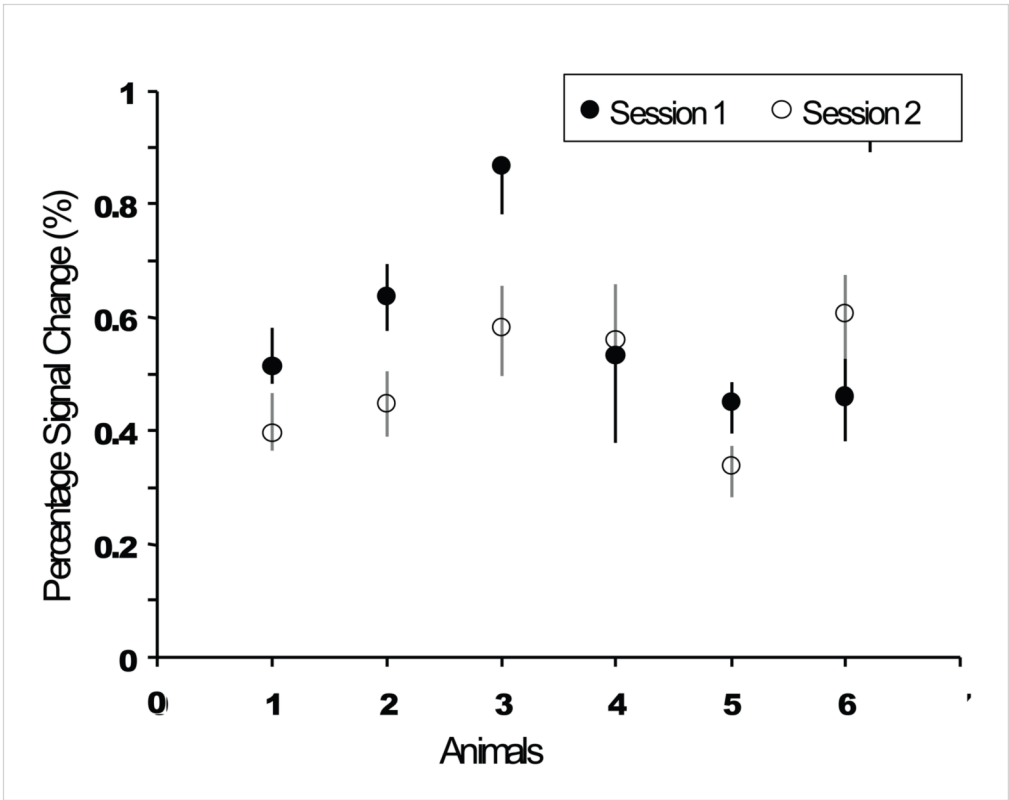

Figure 6.
Summary of peak percentage signal changes (mean ± SD) across animals, imaging runs and sessions.

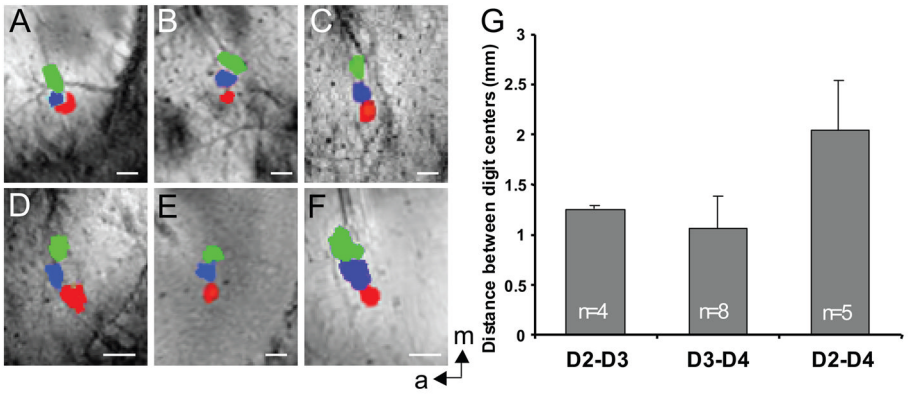

Figure 7.

Variation in fingerpad somatotopy across animals. The composite activation maps of D2 (red), D3 (blue) and D4 (green) showed similar but distinct topographic organization in six monkeys (A–F). The distances between the activation centers of adjacent and non-adjacent digits were calculated across animals and sessions (G). White scale bar indicate 1mm scale. a: anterior; m: middle. Error bars: standard deviation.